[239] Harrington, E. A.; Bebbington, D.; Moore, J.; Rasmussen, R. K.; Ajose-Adeogun, A. O.; Nakayama, T.; Graham, J. A.; Demur, C.; Hercend. T.; Diu-Hercend, A.; Su, M.; Golec, J. M.; Miller, K. M. *Nat. Med.* **2004**, *10*, 262.
[240] Ladygina, N. G.; Latsis, R. V.; Yen, T. *Biomed. Khim.* **2005**, *51*, 170.
[241] Sessa, F.; Mapelli, M.; Ciferri, C.; Tarricone, C.; Areces, L. B.; Schneider, T. R.; Stukenberg, P. T.; Musacchio, A. *Mol. Cell* **2005**, *18*, 379.
[242] Zhu, W. G.; Otterson, G. A. *Curr. Med. Chem. Anti-Canc. Agents* **2003**, *3*, 187.
[243] Zhang, Y. *Genes Dev.* **2003**, *17*, 2733.
[244] Shiio, Y.; Eisenman, R. N. *Proc. Natl. Acad. Sci. U.S.A.* **2003**, *100*, 13225.
[245] Niedergang, C. P.; de Murcia, G.; Ittel, M. E.; Pouyet, J.; Mandel, P. *Eur. J. Biochem.* **1985**, *146*, 185.
[246] Liu, Z.; Oughtred, R.; Wing, S. S. *Mol. Cell. Biol.* **2005**, *25*, 2819.
[247] Kun, E.; Kirsten, E.; Ordahl, C. P. *J. Biol. Chem.* **2002**, *277*, 39066.

Received: October 20, 2005 **Revised: December 29, 2005** **Accepted: January 3, 2006**

Rational Design of Non-Hydroxamate Histone Deacetylase Inhibitors

Takayoshi Suzuki* and Naoki Miyata*

Graduate School of Pharmaceutical Sciences, Nagoya City University, 3-1 Tanabe-dori, Mizuho-ku, Nagoya, Aichi 467-8603, Japan

Abstract: While most inhibitors of histone deacetylases (HDACs) are hydroxamic acid derivatives, several non-hydroxamates have recently been developed as inhibitors and attracted quite a deal of attention. In this review, we present the rational design, inhibitory effect and antiproliferative activity of non-hydroxamate HDAC inhibitors.

Keywords: Histone deacetylase, inhibitor, hydroxamic acid, non-hydroxamate, zinc enzyme, rational drug design, anticancer agent.

INTRODUCTION

In eukaryotes, genetic information is packed in a higher order structure called the chromatin. The fundamental building blocks of chromatin are nucleosomes where genomic DNA is wrapped tightly around core histones [1, 2]. Post-transcriptional modifications of the histones are associated with alterations of chromatin structure that can effect gene expression [3]. The motion that gene expression is regulated by modifications to histones, the so called "histone-code hypothesis" [4, 5], is based on the assumption that these modifications create a specific pattern of substitutions. Acetylation is by far the most studied specific histone modification. The acetylation of specific histone lysine residues is catalyzed by histone acetyltransferases (HATs). Histone acetylation is a reversible process that is regulated by the opposing activities of HATs and histone deacetylases (HDACs) (Fig. 1). In general, hyperacetylation of histone lysine residues correlates with transcriptional activation whereas deacetylation relates to transcriptional silencing [6-9].

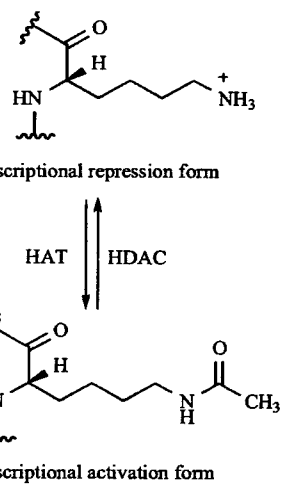

Fig. (1). Reversible acetylation of specific histone lysine residues.

*Address correspondence to these authors at the Graduate School of Pharmaceutical Sciences, Nagoya City University, 3-1 Tanabe-dori, Mizuho-ku, Nagoya, Aichi 467-8603, Japan; Tel/Fax: +81-52-836-3407; E-mail: suzuki@phar.nagoya-cu.ac.jp; miyata-n@phar.nagoya-cu.ac.jp

The inhibition of HDACs causes histone hyperacetylation and leads to the transcriptional activation of genes such as $p21^{WAF1/CIP1}$ [10], *FAS* and *caspase-3* [11] which are associated with cell cycle progression, differentiation or tumorigenesis. Therefore, HDAC inhibitors have emerged as a new generation of anticancer agents. Indeed, HDAC inhibitors such as suberoylanilide hydroxamic acid (SAHA) [12] (Fig. 2) are currently in phase III clinical trials for the treatment of cancer. To date, a number of structurally diverse HDAC inhibitors have been reported [13-18]. To the best of our knowledge, previously reported HDAC inhibitors predominantly rely on hydroxamic acid structures like SAHA, Trichostatin A (TSA) [19, 20] and 3-(4-aroyl-1*H*-2-pyrrolyl)-*N*-hydroxy-2-propenamides such as **1** and **2** [21] (Fig. 2) to achieve the desired effect. However, hydroxamic acids are often poorly absorbed *in vivo* and carry potential metabolic liabilities such as glucoronidation and sulfation [22, 23]. Furthermore, many hydroxamates are prone to hydrolysis *in vivo* giving hydroxylamine which has potential mutagenic properties [24]. Thus, there has been considerable interest in developing non-hydroxamate HDAC inhibitors. Until very recently, known non-hydroxamate HDAC inhibitors were small fatty acids such as sodium butyrate and valproic acid, and *o*-aminoanilides such as MS-275 (Fig. 3) [25-34]. However, most of these are less potent than hydroxamates. Therefore, we and others have searched for replacements for hydroxamic acid with the goal of producing new drugs as well as finding new tools for biological research, and have identified several non-hydroxamate HDAC inhibitors [35-44]. In this review, the rational design and biological activity of non-hydroxamate HDAC inhibitors are presented.

THREE-DIMENSIONAL STRUCTURE AND CATALYTIC MECHANISM OF HDAC

In 1999, Finnin and co-workers published the X-ray crystal structure of an archaebacterial HDAC homologue (HDAC-like protein, HDLP)/SAHA or TSA [45]. It was revealed that the enzyme contains a zinc ion at the bottom of its active site and that the hydroxamic acid group coordinates the zinc ion through its CO and OH groups and also forms three hydrogen bonds between its CO, NH and OH groups and Tyr 297, His 132 and His 131, respectively (Fig. 4). The disclosure has led to a solid understanding of not only the three-dimensional structure of the active site of HDACs but

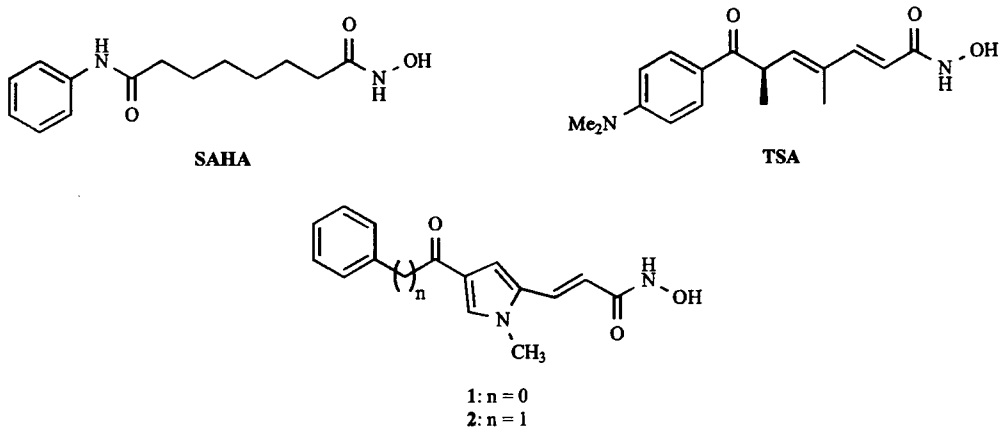

Fig. (2). Hydroxamate HDAC inhibitors.

also the catalytic mechanism for the deacetylation of acetylated lysine substrates. The proposed mechanism is depicted in Fig. **5**. The carbonyl oxygen of the substrate could bind the zinc, and the carbonyl could be located adjacent to the water molecule that chelates the zinc ion. The carbonyl carbon, which becomes a better electrophile through its chelation with the zinc ion, could be attacked by the water molecule activated by His 140 (HDAC1 numbering) and the zinc ion. The nucleophilic attack would result in a tetrahedral carbon-containing transition state, which could be stabilized by two zinc-oxygen interactions and by a hydrogen bond from the Tyr 303 hydroxyl group. In the final step, a proton transfer from His 141 to the nitrogen of the intermediate would trigger the scission of the carbon-nitrogen bond and yield the acetate and lysine products. The crystal structures of human HDAC8 complexed with hydroxamic acid inhibitors, reported recently [46, 47], also supported such a catalytic mechanism of HDACs.

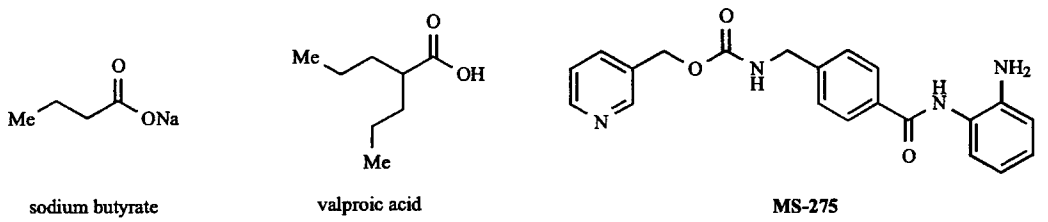

Fig. (3). Structures of sodium butyrate, valproic acid and MS-275.

MOLECULAR DESIGN OF NON-HYDROXAMATE HDAC INHIBITORS

Structure-Based Drug Design

On the basis of the three-dimensional structure of the active site of the enzyme, SAHA-based non-hydroxamates were designed and synthesized as HDAC inhibitors (Fig. **6**). As mentioned above, the co-crystal structure of HDLP/hydroxamate or HDAC8/hydroxamate made it clear that the hydroxamic acid group chelates the zinc ion in a bidentate fashion and forms hydrogen bonds with tyrosine and two histidines [45-47] (Fig. **7a**). As bidentate zinc-binding groups (ZBGs), we designed SAHA-based hydroxyurea (**3**), semicarbazide (**4**) and hydroxysulfonamide (**5**) [35, 38], which could coordinate the zinc ion bidentately and could also form hydrogen bonds with tyrosine and two histidines like hydroxamic acid (Fig. **7b**). We also designed monodentate ZBGs. Thiol **6**, thioacetate **7** and methylsulfide **8** were designed based on the high thiophilicity of zinc ion [36, 38]. In particular, thiol could interact not only with zinc ion but with amino acid residues in the active site. Another newly designed mondentate ZBG is sulfoxide (**9**) [39]. Since sulfoxide has a partial negative charge on its oxygen, it is estimated to chelate zinc ion and inhibit HDACs. Irreversible HDAC inhibitors were also designed based on the three-

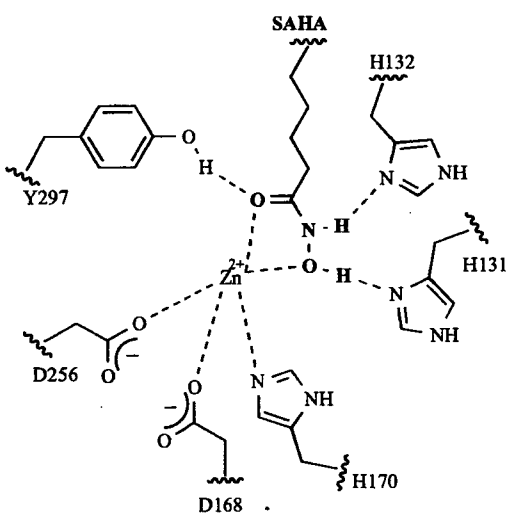

Fig. (4). SAHA in the catalytic core of HDLP.

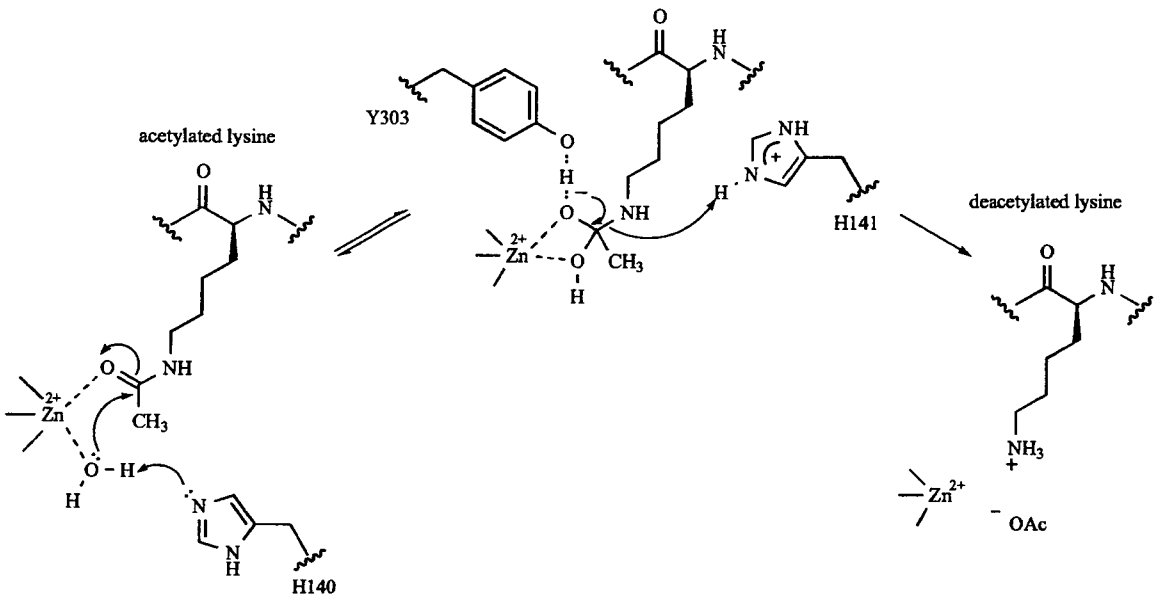

Fig. (5). Proposed catalytic mechanism for the deacetylation of acetylated lysine.

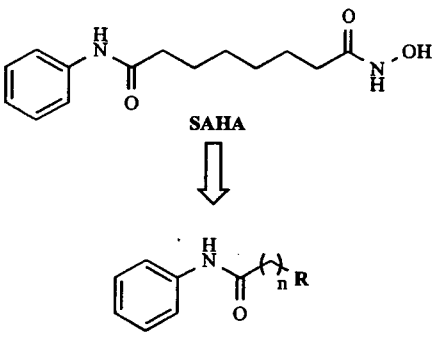

3 : R = -NHCONHOH, n = 5
4 : R = -NHCONHNH$_2$, n = 5
5 : R = -SO$_2$NHOH, n = 6
6 : R = -SH, n = 6
7 : R = -SAc, n = 6
8 : R = -SMe, n = 6
9 : R = -S(O)Me, n = 6
10: R = -NHCH$_2$CÂfiCH, n = 6
11: R = -N(CH$_2$CÂfiCH)$_2$, n = 6
12: R = -NHCOCH$_2$Br, n = 6
13: R = 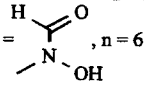 , n = 6

Fig. (6). SAHA-based non-hydroxamate compounds designed based on the three-dimensional structure of HDAC.

dimensional structure of the active site of HDLP or HDAC8. As described above, the crystal structures of the HDLP/hydroxamate and HDAC8/hydroxamate complexes revealed that the active site of HDACs is constructed mainly from nucleophilic amino acids such as histidine and asparatic acid [45-47]. Since the imidazole group of histidine and the carboxylate anion of asparatic acid are able to react with electrophiles, we designed analogues bearing propargyl amino (**10**, **11**) and bromoacetamide (**12**) which could form covalent bonds with histidines or asparatic acids of the enzyme [35, 38]. Schultz and co-workers also designed *N*-formyl hydroxylamine **13** on the basis of the co-crystal structure of HDLP/SAHA or HDLP/TSA [40]. Compounds bearing *N*-formyl hydroxylamine could inhibit HDACs by forming a bidentate chelate with the zinc ion in the active site of HDACs.

Mai and co-workers designed several non-hydroxamates based on the structure of **1** or **2**, hydroxamate HDAC inhibitors identified by them (Fig. **8**) [21]. Some hydroxamic acid-like derivatives **14**–**22** bearing *O*-methylhydroxamate (**14**), hydrazine (**15**), 2-hydroxyethylamide (**16**), *o*-hydroxyanilide (**17**), monophosphonic acid (**18**), nitrile (**19**), barbiturate (**20**), thiobarbiturate (**21**) and amidine (**22**) moieties are able to chelate the zinc ion and are expected to inhibit HDACs.

Mechanism-Based Drug Design

We and other groups designed SAHA-based non-hydroxamates based on the proposed catalytic mechanism for the deacetylation of acetylated lysine residues (Fig. **9**). We initially designed substrate analogues based on the proposed deacetylation mechanism whereby a zinc-chelating water molecule activated by histidine makes a nucleophilic attack on the carbonyl carbon of an acetylated lysine substrate (Fig. **10a**) [45-47]. With this mechanism, the HDACs would supposedly be inhibited if the water molecule is forcibly removed from the zinc ion, and then heteroatom-containing substrate analogues **23**–**26** were designed [37, 38]. These analogues would be recognized as substrates by HDACs and be easily taken into the active site where they would force the water molecule off the zinc ion and the reactive site for deacetylation through chelation of the heteroatom to the zinc ion, and behave as HDAC inhibitors (Fig. **10b**).

The other design was based on the transition state (TS) structure of HDAC deacetylation, which was estimated to include a tetrahedral carbon [45-47] (Fig. **11a**) as with other zinc proteases [48]. TS analogue inhibitors were designed

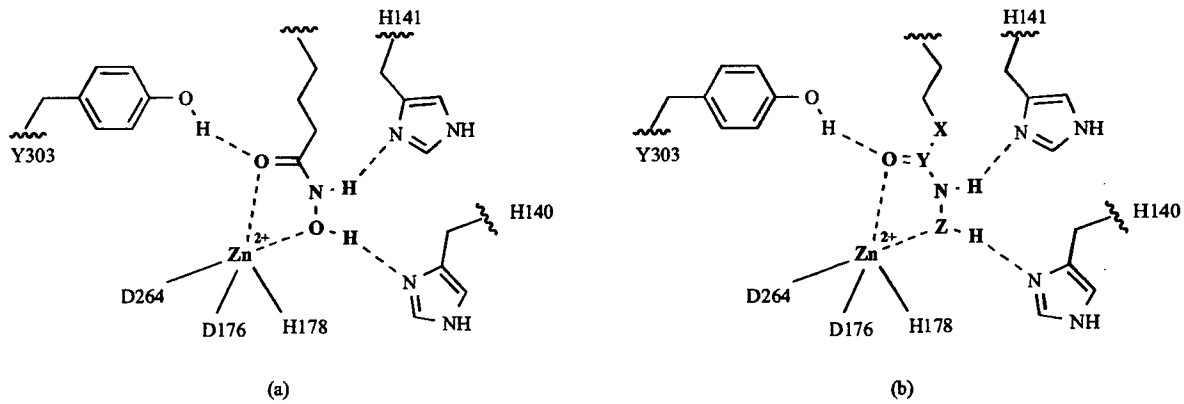

Fig. (7). Model for the binding of SAHA (a) and hydroxamic acid mimics **3–5** in the catalytic core of HDAC1.

independently by us [37, 38] and Etzkorn *et al* [49]. Phosphone- and sulfone-based SAHA analogues could be TS analogue inhibitors because they have sufficient similarity with the TS of amide bond hydrolysis (Fig. **11b** and **11c**), both from a steric and an electronic point of view [50]. Then, compounds **27–31**, in which a hydroxamic acid of SAHA is replaced by sulfonamide, sulfone, phosphonamidate, phosphonate and phosphinate, respectively, were designed as TS analogues. Frey and co-workers at Abbott designed electrophilic ketones such as **32** and **33** [41-44]. The hydrated form of electrophilic ketones could act as a TS analogue and coordinate the zinc ion in the active site of HDACs [51] (Fig. **11d**).

ENZYME INHIBITORY ACTIVITY

Compounds **3–33** were tested with an *in vitro* enzyme assay. Compound **34** [32], where the hydroxamic acid of SAHA is replaced with *o*-aminoanilide, was prepared and tested as a reference compound. The results are summarized in Tables **1-3**.

Table **1** shows the inhibitory activity toward human HDACs of SAHA-based non-hydroxamates **3-13** designed based on the three-dimensional structure of HDAC. The IC_{50} values of SAHA and *o*-aminoanilide **34** were 0.28 μM and 120 μM, respectively. Among newly synthesized compounds **3–5**, which were designed as compounds with bidentate

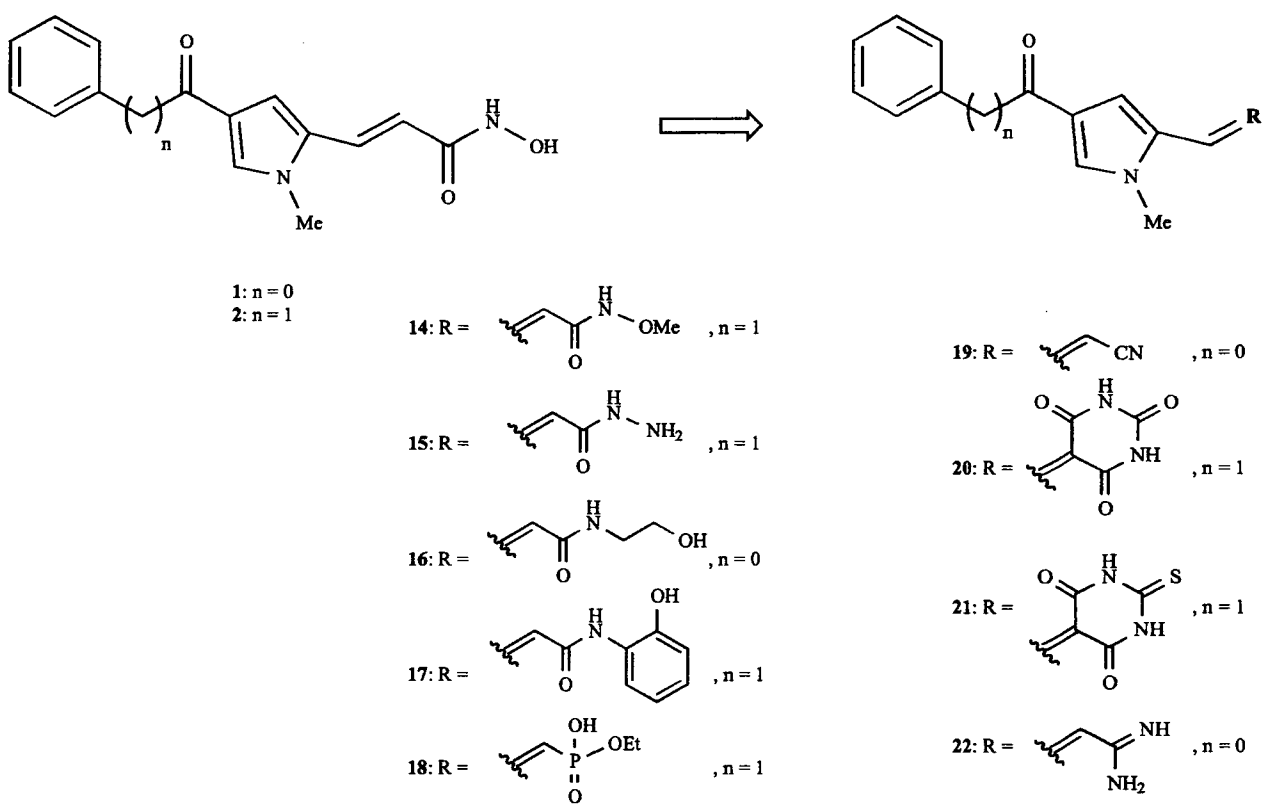

Fig. (8). Non-hydroxamates designed based on the structure of **1** or **2**.

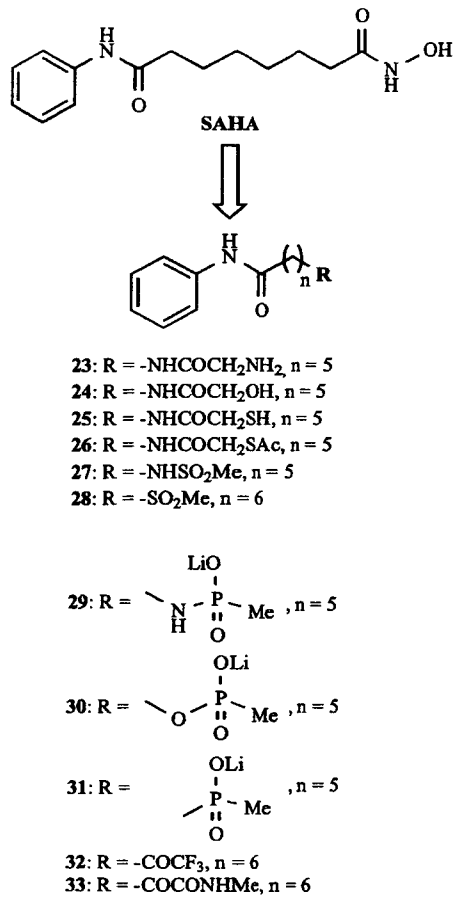

Fig. (9). SAHA-based non-hydroxamates designed based on the catalytic mechanism for the deacetylation of acetylated lysine substrates.

ZBGs, hydroxyurea **3** and semicarbazide **4** showed inhibitory activity although they were much less effective than SAHA [35, 38]. As to the compounds with monodentate ZBGs (**6–9**), the activity of thiol **6** was far greater than expected. Although the inhibitory ability of monodentate ZBGs was thought to be less than that of bidentate ZBGs such as hydroxamic acid, a pronounced inhibitory effect

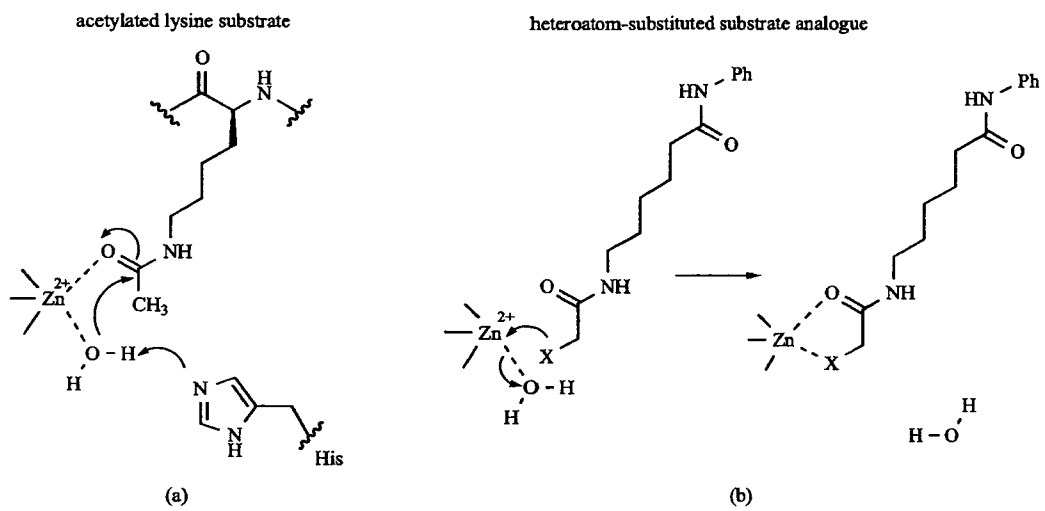

Fig. (10). Mechanism proposed for the deacetylation of acetylated lysine substrate (a), and model for the binding of hetero atom-containing substrate analogues to zinc ion (b).

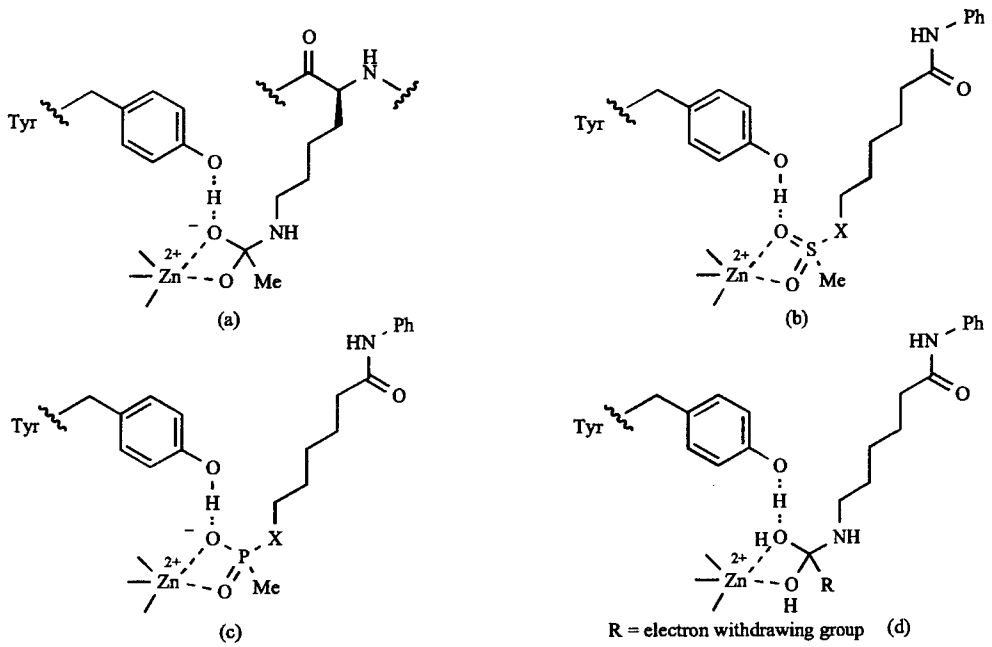

Fig. (11). Transition state proposed for HDACs (a), and models for the binding of sulfone derivatives (b), phosphone derivatives (c) and hydrated electrophilic ketones (d).

Table 1. HDAC Inhibition Data for SAHA and SAHA-Based Non-Hydroxamtes 3–13 and 34 [35, 38, 40]

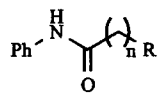

Compd.	R	*n*	IC_{50} (μM)[a]
SAHA	–CONHOH	6	0.28
34	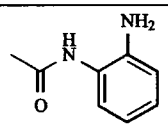	6	120
3	–NHCONHOH	5	80
4	$-NHCONHNH_2$	5	150
5	$-SO_2NHOH$	6	> 100
6	–SH	6	0.21
7	–SAc	6	7.1
8	–SMe	6	> 100
9	–S(O)Me	6	48
10	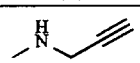	6	> 100
11	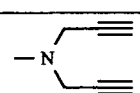	6	> 100
12	$-NHCOCH_2Br$	6	14
13	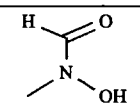	6	4.0[b] / 11[c]

[a]Activity against a mixture of HDACs in HeLa nuclear extracts. [b]Activity against HDAC2. [c] Activity against HDAC8.

(IC_{50} = 0.21 μM) was observed with thiol **6** [36, 38], which was much more active than *o*-aminoanilide **34** and as potent as SAHA. The transformation of thiol into thioacetate (**7**) and methylsulfide (**8**) led to an inhibitor that was about 30-fold less potent and a compound devoid of anti-HDAC activity, respectively. These results suggest that the thiolate anion generated under physiological conditions is intimately involved in the interaction with the zinc ion in the active site. In addition, sulfoxide **9**, the other compound with a monodentate ZBG, inhibited HDACs with an IC_{50} of 48 μM [39]. Of the three compounds designed as irreversible HDAC inhibitors (**10–12**), bromoacetamide **12** exhibited an IC_{50} of 14 μM and its activity was about 9-fold as strong as that of *o*-aminoanilide **34**, but much weaker than that of SAHA [35, 38]. *N*-Formyl hydroxylamine **13** was reported by Schultz *et al* to inhibit HDAC2 and HDAC8 with IC_{50}s of 11 μM and 4.0 μM, respectively [40].

Another series of non-hydroxamates **14–22** were evaluated for their inhibitory activity against maize histone deacetylase HD2 (Table **2**). Among these compounds, nitrile **19** and amidine **22** displayed anti-HDAC activity with IC_{50}s of 27 μM and 23 μM, respectively, although they were 6- to 7-fold less potent than their reference compound **1** [21].

Table **3** shows the inhibitory activity toward human HDACs of SAHA-based non-hydroxamates **23-33** designed based on the catalytic mechanism for the deacetylation of acetylated lysine substrate. We initially investigated the inhibitory activity of hetero atom-containing substrate analogues **23–26**. Potent inhibition was observed with mercaptoacetamide **25**, while aminoacetamide **23** and hydroxyacetamide **24** did not possess inhibitory activity [37, 38]. Mercaptoacetamide **25** exhibited an IC_{50} of 0.39 μM, and its activity greatly surpassed that of *o*-aminoanilide **34** and was comparable to that of SAHA. As expected, the

Table 2. HDAC Inhibition Data for 1, 2 and 14–22 [21]

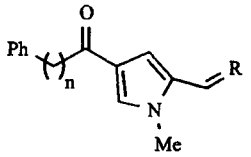

Compd.	R	*n*	IC_{50} (μM)[a]
1	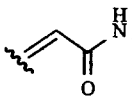	0	3.8
2	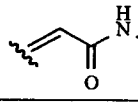	1	0.1
14	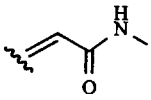	1	NI[b]
15	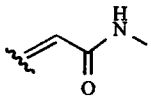	1	> 30[c]
16	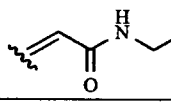	0	> 30[d]
17	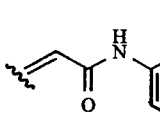	1	NI
18	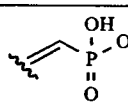	1	NI
19		0	27
20	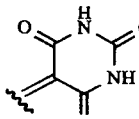	1	100
21	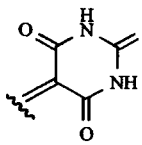	1	85
22	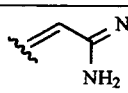	0	23

[a]Activity against maize HD2. [b]NI = no inhibition at 30 μM. [c]0.2% inhibition at 33.8 μM. [d]0.9% inhibition at 30.5 μM.

transformation of thiol into thioacetate (**26**) led to a much less potent inhibitor. These results suggest that the ease of ionization of thiol is an important factor in the inhibition of HDACs like the case of thiol **6**. Among TS analogues, electrophilic ketones **32** and **33** showed significant inhibitory activity (IC_{50} of **32** = 6.7 μM, IC_{50} of **33** = 0.34 μM), whereas sulfone derivatives **27** and **28**, and phosphorus analogues **29**, **30** and **31** were found to be less potent inhibitors [37, 38, 41-44, 49].

Table 3. HDAC Inhibition Data for SAHA and SAHA-Based Non-Hydroxamtes 23–34 [37, 38, 41, 42, 49]

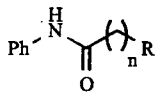

Compd.	R	*n*	IC_{50} (μM)[a]
SAHA	–CONHOH	6	0.28
34	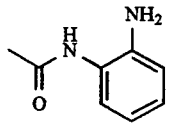	6	120
23	$-NHCOCH_2NH_2$	5	> 100
24	$-NHCOCH_2OH$	5	> 100
25	$-NHCOCH_2SH$	5	0.39
26	$-NHCOCH_2SAc$	5	22
27	$-NHSO_2Me$	5	7500
28	$-SO_2Me$	6	230
29	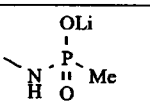	5	570
30	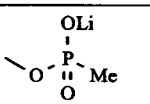	5	6100
31	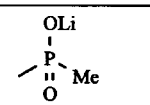	5	6100
32	$-COCF_3$	6	6.7[b]
33	–COCONHMe	6	0.34[b]

[a]Activity against a mixture of HDACs in HeLa nuclear extracts. [b]Activity against a mixture of HDAC1 and HDAC2.

We also studied the mechanism by which thiol **6** and mercaptoacetamide **25** inhibit HDACs in greater detail [37, 38]. Although the sulfhydryl group of **6** and the mercaptoacetamide group of **25** were designed to chelate zinc ion, it is possible that they inhibit HDACs by forming a covalent disulfide bond with cysteine residues on these enzymes. We examined this possibility using a Lineweaver-Burk plot. First, a kinetic enzyme assay was carried out using compound **6** (Fig. **12**). The data from this experiment revealed that thiol **6** engages in competitive inhibition with acetylated lysine substrates, with an inhibition constant (*Ki*) of 0.11 μM. Since cysteine is not a component of the active site of HDACs, the sulfhydryl group of **6** likely interacts with the zinc in the active site. Since thiol **6** proved to be a competitive inhibitor and to act within the active center of HDACs, its mode of binding within this site was studied. The low energy conformation of **6** was calculated when

docked in the model structure based on the X-ray crystal data of HDAC8 using Macromodel 8.1 software. An inspection of

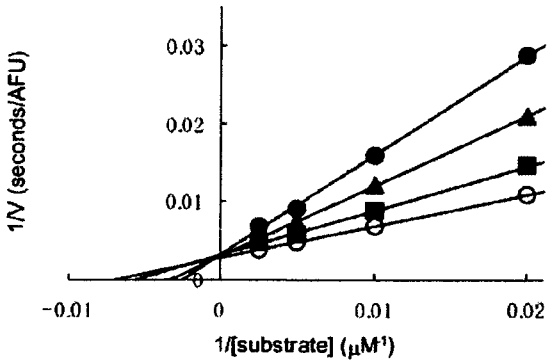

Fig. (12). Reciprocal rate *vs* reciprocal acetylated lysine substrate concentration in the presence of 0.3 (●), 0.1 (▲), 0.03 (■), and 0 (○) μM of **6**.

the HDAC8/**6** complex shows that the sulfur atom of **6** was located 2.35 Å from the zinc ion, 2.24 Å from the OH group of Tyr 306, and 2.66 Å from a water molecule which forms a hydrogen bond with the imidazole group of His142 (Fig. **13**). These results suggest that thiol **6** strongly inhibits HDACs by interacting directly with zinc ion, Tyr 306, and His 142 *via* a water molecule.

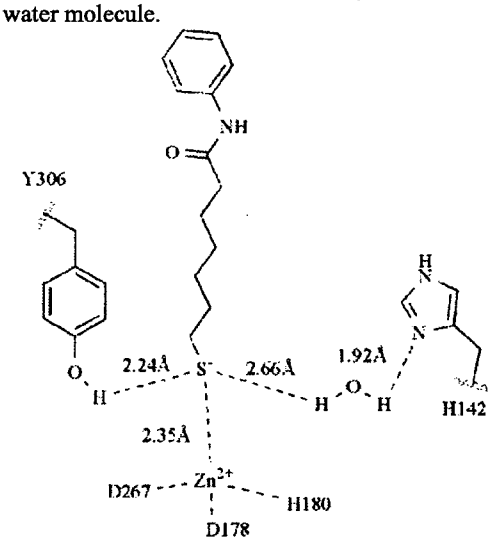

Fig. (13). Low energy conformation of **6** docked in the HDAC8 catalytic core.

Next, a Lineweaver-Burk plot was drawn for mercaptoacetamide **25** (Fig. **14**). Compound **25** turned out to be an inhibitor competitive with acetylated lysine substrates (*Ki* = 0.78 μM). The low energy conformation of **25** docked in the catalytic core of HDAC8 was also calculated. It was found that the sulfur atom and oxygen atom of **25** were located 2.44 Å and 2.04 Å from the zinc ion, respectively, and that a water molecule, which is required for the deacetylation of acetylated lysine substrates, was positioned 4.95 Å apart from the zinc ion (Fig. **15**). This calculation suggests that **25** inhibits HDACs by chelating the zinc ion in a bidentate fashion through its sulfur and oxygen atoms, and by removing a water molecule from the zinc and the reactive site for the deacetylation, without being hydrolyzed by HDACs.

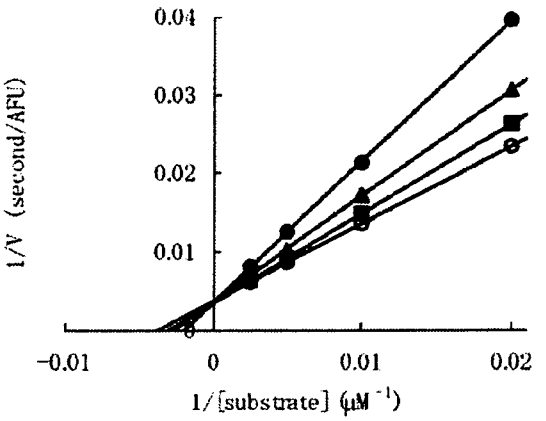

Fig. (14). Reciprocal rate *vs* reciprocal acetylated lysine substrate concentration in the presence of 1 (●), 0.3 (▲), 0.1 (■), and 0 (○) μM of **25**.

Based on the results shown in Tables **1-3**, we selected thiol **6** and further studied its structure-activity relationship in an *in vitro* assay using a HeLa nuclear extract rich in HDAC activity, because it showed the strongest activity of all non-hydroxamates [37, 38]. First, the effect of the linker parts of thiol **6** was examined. The results are shown in Table **4**. The inhibition of HDACs was distinctly dependent on chain length, with $n = 7$ (**35**) and $n = 4$ (**37**) resulting in less potent inhibitors. However, compound **36**, in which $n = 5$, proved to be equally effective as **6**, in which $n = 6$. As for the group attaching to the phenyl moiety, ether **38** displayed moderate activity, whereas the activity of the reversed amide **39** was sustained. Next, the aromatic cap part was examined (Table **5**). Considering that the entrance of the *N*-acetylated lysine binding channel is composed mainly of aromatic amino acids such as tyrosine and phenylalanine [45-47], we replaced the phenyl group of **6** or **39** with various aromatic

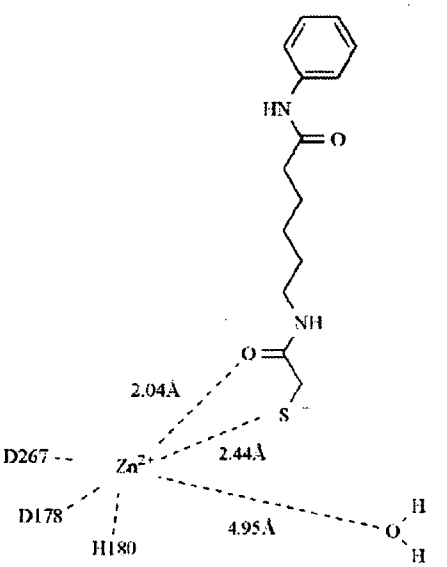

Fig. (15). Low energy conformation of **25** docked in the HDAC8 catalytic core.

Table 4. Effect of Linker Variation on Inhibitory Activity of Thiols [35, 38]

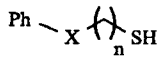

Compd.	X	*n*	IC_{50} (μM)
6	–NHCO–	6	0.21
35	–NHCO–	7	1.5
36	–NHCO–	5	0.37
37	–NHCO–	4	6.2
38	–O–	6	11
39	–CONH–	6	0.36

groups, which were expected to have higher affinity for HDACs through π-π interaction or hydrophobic interaction. In the amide-linked series, 4-substituted phenyl compounds tended to be less active. Specifically, compounds **40** (Ar = 4-NMe_2-Ph), **41** (Ar = 4-biphenyl) and **43** (Ar = 4-PhO-Ph) were about 3- to 6-fold less potent inhibitors than the parent thiol **6**. On the other hand, 3-biphenyl **42** showed a 3-fold increase in inhibitory activity (IC_{50} of 0.075 μM). In addition, 3-phenoxy compound **44** was as active as compound **6**. We also investigated the effect of heteroaryl rings. Changing the phenyl group to a 3-pyridine ring (**45**), 4-phenyl-2-thiazole ring (**47**), and 2-benzothiazole ring (**48**) maintained or slightly reduced the activity, whereas 3-quinoline **46** had improved activity (IC_{50} of 0.072 μM). The reverse amide-linked series were at least as active as the parent thiol **39**, with the exception of **49** (Ar = 4-NMe_2-Ph), which was a slightly less potent inhibitor. In particular, the reversed amides **50** with 2-naphthalene and **51** with 2-benzofuran exhibited about a 3-fold increase in potency (IC_{50}s of 0.085 μM and 0.079 μM, respectively). As a result, IC_{50}s in the double-digit nanomolar range were observed with 3-biphenyl **42**, 3-quinoline **46**, 2-naphthalene **50**, and 2-benzofuran **51**, which were approximately 3- to 4-fold more potent than SAHA.

ANTIPROLIFERATIVE ACTIVITY

To confirm the effectiveness of thiol-based HDAC inhibitors as anticancer drugs and tools for biological research, the antiproliferative activity of thiol **6** was examined using human lung cancer NCI-H460 cells [38]. However, compound **6** was found to be only weakly active (Table **6**), although **6** was highly active in an enzyme assay. The reason for the weak activity of thiol **6** is unclear, but it is likely due to poor membrane permeability resulting from the highly polar character of this compound. To improve its permeability and its ability to inhibit cancer cell growth, a transient masking of the sulfhydryl group, a prodrug approach, was investigated. As a prodrug of thiol **6**, we prepared disulfide **53**, which was expected to be reduced to release the free thiol **6** in the cellular environment. However, disulfide **53** failed to exhibit a growth inhibitory effect on NCI-H460 cells. Next, we prepared compound **7**, an acetyl derivative of thiol **6**. Compound **7** proved to be relatively

Table 5. Effect of Aromatic Group on Inhibitory Activity of Thiols [35, 38]

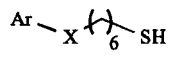

Compd.	Ar	X	IC_{50} (μM)
6	–Ph	–NHCO–	0.21
40	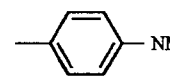	–NHCO–	1.2
41	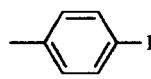	–NHCO–	1.1
42	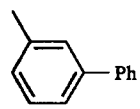	–NHCO–	0.075
43	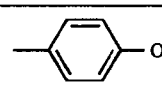	–NHCO–	0.62
44	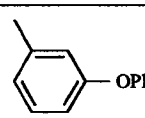	–NHCO–	0.21
45	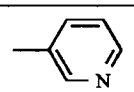	–NHCO–	0.11
46	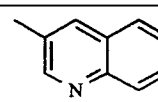	–NHCO–	0.072
47	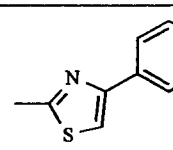	–NHCO–	0.17
48	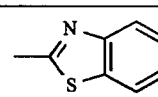	–NHCO–	0.34
39	–Ph	–CONH–	0.36
49	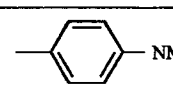	–CONH–	0.61
50	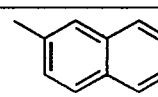	–CONH–	0.085
51	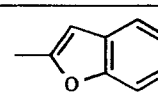	–CONH–	0.079
52	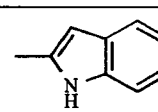	–CONH–	0.1

potent compared with thiol **6** and disulfide **53** (EC_{50} of 36 μM). On the basis of this finding, we prepared other *S*-acyl compounds (**54–61**) and evaluated their antiproliferative activities. Since the ClogP values of compounds **54–61** are 3.71, 4.24, 4.06, 4.41, 3.54, 4.67, 4.69 and 4.65, respectively, and are larger than that of thiol **6** (ClogP of **6** = 3.17), these compounds were expected to permeate cell membrane more efficiently and show higher cellular activity than **6**. This series of compounds exhibited greater potency than thiol **6** and acetyl compound **7**, except for pivaloyl compound **57**, which was a less potent cell growth inhibitor than **7**. Among them, isobutyryl compound **56** showed about a 2-fold increase in activity when compared to acetyl compound **7** (EC_{50} of 20 μM). Since *S*-acyl compounds are weakly active in enzyme assays (e.g. IC_{50} of **56** > 50 μM), they could possibly permeate the cell membrane more efficiently than thiol **6**, and be converted to thiol **6** by enzymatic hydrolysis within the cell [52]. The compound bearing a (pivaloyloxy)methyl group [53] (**62**) was slightly less active than isobutyryl compound **56**. With the results shown in Table **6**, a selected set of active compounds from the enzymatic assay were *S*-isobutyrylated and evaluated for their antiproliferative activities (Table **7**). Changing the phenyl group of compound **56** to other aromatic groups led to positive results. Isobutyryl analogues **63–71** were generally more potent than the parent compound **56**; the sole exception was **64** (Ar = 3-OPh-Ph) which was a less potent compound. Above all, 3-biphenyl (**63**), 3-pyridinyl (**65**) and 4-phenyl-2-thiazolyl (**67**) analogues showed strong activity in inhibiting the growth of NCI-H460 cells, with EC_{50}s of 2–3 μM. Furthermore, we evaluated antiproliferative activities of SAHA and 4-phenyl-2-thiazole **67**, the most potent compound in this study, against nine other human cancer cell lines (Table **8**). Compound **67** strongly inhibited the growth of various human cancer cells, with EC_{50} values ranging from 1 to 10 μM, and these antiproliferative activities were comparable to those of SAHA (average EC_{50} of **67** 3.8 μM, SAHA 3.7 μM) which is currently being evaluated in phase III clinical trials for use in the treatment of cancer.

Table 6. Antiproliferative Effect on NCI-H460 Cells of Compound 6 and its S-Modified Prodrugs [38][a]

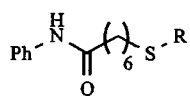

Compd.	R	EC_{50} (μM)
6	–H	>50[b]
53	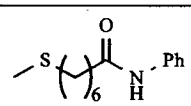	>50[c]
7	–Ac	36
54	–COEt	28
55	–CO*n*-Pr	22
56	–CO*i*-Pr	20
57	–CO*t*-Bu	77
58	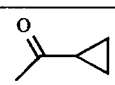	27
59	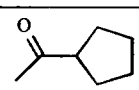	21
60	–Bz	25
61	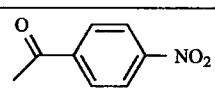	24
62	$–CH_2OCO$*t*-Bu	25

[a]EC_{50} of SAHA =1.1 μM. [b]34% inhibition at 50 μM. [c]10% inhibition at 50 μM.

Table 7. Cell Growth Inhibition Data on NCI-H460 Cells for Compound 56 and its Derivatives [38]

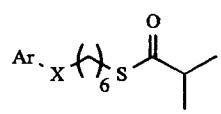

Compd.	Ar	X	EC_{50} (μM)
56	–Ph	–NHCO–	20
63	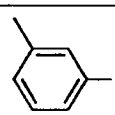	–NHCO–	2.8
64	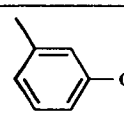	–NHCO–	25
65	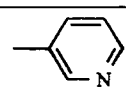	–NHCO–	2.9
66	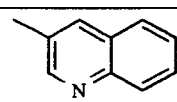	–NHCO–	8.0
67	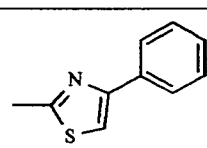	–NHCO–	2.1
68	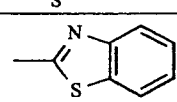	–NHCO–	9.5
69	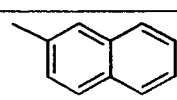	–CONH–	12
70	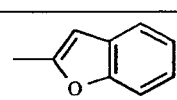	–CONH–	4.1
71	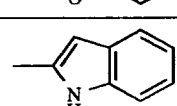	–CONH–	12

Table 8. Growth Inhibition of Various Cancer Cells Using SAHA and Compound 67 [38]

Cell		SAHA	67
		EC_{50} (μM)	EC_{50} (μM)
MDA-MB-231	Breast Cancer	1.5	2.3
SNB-78	Central Nervous System	16	9.1
HCT116	Colon Cancer	0.58	3.0
NCI-H226	Lung Cancer	2.6	2.6
LOX-IMVI	Melanoma	1.3	1.1
SK-OV-3	Ovarian Cancer	2.5	4.5
RXF-631L	Renal Cancer	2.0	2.4
St-4	Stomach Cancer	5.2	5.0
DU-145	Prostate Cancer	1.6	4.5
Mean		3.7	3.8

By Western blot analysis, compound **67** was shown to give rise to elevated and dose-dependent levels of acetylated histone H4 and $p21^{WAF1/CIP1}$ in HCT 116 cells (Fig. **16**). These results suggested that the antiproliferative activity of compound **67** significantly correlates with the inhibition of intracellular HDACs.

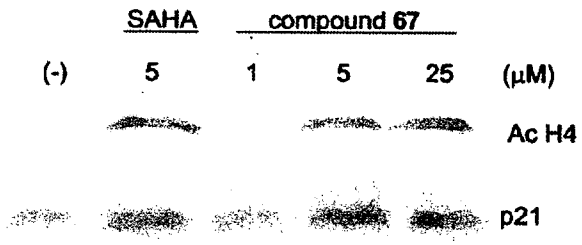

Fig. (16). Western blot analysis of histone hyperacetylation and $p21^{WAF1/CIP1}$ induction in HCT 116 cells produced by compound **67** and by reference compound SAHA. HCT116 cells were incubated with compound **67** for 8 h at 37°C.

PERSPECTIVE

By rational drug design, several new non-hydroxamate structures containing thiols were identified. The discovery of non-hydroxamate inhibitors of HDACs introduced in this review should provide the basis for the development of ideal inhibitors free of the problems associated with hydroxamates.

To date, eleven HDAC isozymes have been identified. Isozyme-selective HDAC inhibitors are considered to be useful not only as tools for probing the biology of HDAC isozymes but as drugs with low toxicity. Interestingly, it has recently been reported that many non-hydroxamate HDAC inhibitors are inactive against HDAC6 [32, 54-57], indicating the significance of the selectivity of non-hydroxamates. Indeed, compound **9**, one of the nonhydroxamates presented in this review, was recently reported to show selectivity, whereas SAHA, a representative hydroxamate, did not discriminate well among the HDAC isozymes [39]. Further study on non-hydroxamate HDAC inhibitors will offer a basis on which to better design isozyme-selective inhibitors and to surmount the problems associated with hydroxamates.

REFERENCES

[1] White, C. L.; Suto, R. K.; Luger, K. *EMBO J.* **2001**, *20*, 5207.
[2] Luger, K. *Curr. Opin. Genet. Dev.* **2003**, *13*, 127.
[3] Berger, S. L. *Curr. Opin. Genet. Dev.* **2002**, *12*, 142.
[4] Strahl, B. D.; Allis, C. D. *Nature* **2000**, *403*, 41.
[5] Izuka, M.; Smith, M. M. *Curr. Opin. Genet. Dev.* **2003**, *13*, 154.
[6] Hassig, C. A.; Schreiber, S. L. *Curr. Opin. Chem. Biol.* **1997**, *1*, 300.
[7] Kouzarides, T. *Curr. Opin. Genet. Dev.* **1999**, *9*, 40.
[8] Grozinger, C. M.; Schreiber, S. L. *Chem. Biol.* **2002**, *9*, 3.
[9] Taunton, J.; Hassig, C. A.; Schreiber, S. L. *Science* **1996**, *272*, 408.
[10] Sambucetti, L. C.; Fischer, D. D.; Zabludoff, S.; Kwon, P. O.; Chamberlin, H.; Trogani, N.; Xu, H.; Cohen, D. *J. Biol. Chem.* **1999**, *274*, 34940.
[11] Klisovic, D. D.; Katz, S. E.; Effron, D.; Klisovic, M. I.; Wickham, J.; Parthun, M. R.; Guimond, M.; Marcucci, G. *Invest. Ophth. Vis. Sci.*, **2003**, *44*, 2390.
[12] Richon, V. M.; Webb, Y.; Merger, R.; Sheppard, T.; Jursic, B.; Ngo, L.; Civoli, F.; Breslow, R.; Rifkind, R. A.; Marks, P. A. *Proc. Natl. Acad. Sci. U.S.A.* **1996**, *93*, 5705.
[13] Jung, M. *Curr. Med. Chem.* **2001**, *8*, 1505.
[14] Arts, J.; de Schepper, S.; Van Emelen, K. *Curr. Med. Chem.* **2003**, *10*, 2342.
[15] Yoshida, M.; Matsuyama, A.; Komatsu, Y.; Nishino, N. *Curr. Med. Chem.* **2003**, *10*, 2351.
[16] Miller, T. A.; Witter, D. J.; Belvedere, S. *J. Med. Chem.* **2003**, *46*, 5097.
[17] Monneret, C. *Eur. J. Med. Chem.* **2005**, *40*, 1.
[18] Mai, A.; Massa, S.; Rotili, D.; Cerbara, I.; Valente, S.; Pezzi, R.; Simeoni, S.; Ragno, R. *Med. Res. Rev.* **2005**, *25*, 261.
[19] Yoshida, M.; Horinouchi, S.; Beppu, T. *BioEssays* **1995**, *17*, 423.
[20] Vanhaecke, T.; Papeleu, P.; Elaut, G.; Rogiers, V. *Curr. Med. Chem.* **2004**, *11*, 1629.
[21] Mai, A.; Massa, S.; Ragno, R.; Cerbara, I.; Jesacher, F.; Loidl, P.; Brosch, G. *J. Med. Chem.* **2003**, *46*, 512.
[22] Mulder, G. J.; Meerman, J. H. *Environ. Health Perspect.* **1983**, *49*, 27.
[23] Vassiliou, S.; Mucha, A.; Cuniasse, P.; Georgiadis, D.; Lucet-Levannier, K.; Beau, F.; Kannan, R.; Murphy, G.; Knaeuper, V.; Rio, M. C.; Basset, P.; Yiotakis, A.; Dive, V. *J. Med. Chem.* **1999**, *42*, 2610.
[24] Whittaker, M.; Floyd, C. D.; Brown, P.; Gearing, A. J. *Chem. Rev.* **1999**, *99*, 2735.
[25] Chen, J. S.; Faller, D. V. *Curr. Cancer Drug Targets* **2003**, *3*, 219.
[26] Gottlicher, M.; Minucci, S.; Zhu, P.; Kramer, O. H.; Schimpf, A.; Giavara, S.; Sleeman, J. P.; Lo Coco, F.; Nervi, C.; Pelicci, P. G.; Heinzel, T. *EMBO J.* **2001**, *20*, 6969.
[27] Phiel, C. J.; Zhang, F.; Huang, E. Y.; Guenther, M. G.; Lazar, M. A.; Klein, P. S. *J. Biol. Chem.* **2001**, *276*, 36734.
[28] Lea, M. A.; Sura, M.; desBordes, C. *Cancer Chemo. Pharm.* **2004**, *54*, 57.
[29] Warrell, R. P.; He, L.; Richon, V.; Calleja, E.; Pandolfi, P. P.; *J. Natl. Cancer Inst.* **1998**, *90*, 1621.
[30] McLaughlin, F.; La Thangue, N. B. *Biochem. Pharmacol.* **2004**, *68*, 1139.
[31] Suzuki, T.; Ando, T.; Tsuchiya, K.; Fukazawa, N.; Saito, A.; Mariko, Y.; Yamashita, T.; Nakanishi, O. *J. Med. Chem.* **1999**, *42*, 3001.
[32] Wong, J. C.; Hong, R.; Schreiber, S. L. *J. Am. Chem. Soc.* **2003**, *125*, 5586.
[33] Vaisburg, A.; Bernstein, N.; Frechette, S.; Allan, M.; Abou-Khalil, E.; Leit, S.; Moradei, O.; Bouchain, G.; Wang, J.; Woo, S. H.; Fournel, M.; Yan, P. T.; Trachy-Bourget, M. C.; Kalita, A.; Beaulieu, C.; Li, Z.; MacLeod, A. R.; Besterman, J. M.; Delorme, D. *Bioorg. Med. Chem. Lett.* **2004**, *14*, 283.
[34] Bouchain, G.; Delorme, D. *Curr. Med. Chem.* **2003**, *10*, 2359.

[35] Suzuki, T.; Nagano, Y.; Matsuura, A.; Kohara, A.; Ninomiya, S.; Kohda, K.; Miyata, N. *Bioorg. Med. Chem. Lett.* **2003**, *13*, 4321.
[36] Suzuki, T.; Kouketsu, A.; Matsuura, A.; Kohara, A.; Ninomiya, S.; Kohda, K.; Miyata, N. *Bioorg. Med. Chem. Lett.* **2004**, *14*, 3313.
[37] Suzuki, T.; Matsuura, A.; Kouketsu, A.; Nakagawa, H.; Miyata, N. *Bioorg. Med. Chem. Lett.* **2005**, *15*, 331.
[38] Suzuki, T.; Nagano, Y.; Kouketsu, A.; Matsuura, A.; Maruyama, S.; Kurotaki, M.; Nakagawa, H.; Miyata, N. *J. Med. Chem.* **2005**, *48*, 1019.
[39] Suzuki, T.; Matsuura, A.; Kouketsu, A.; Hisakawa, S.; Nakagawa, H.; Miyata, N. *Bioorg. Med. Chem.* **2005**, *13*, 4332.
[40] Wu, T. Y. H.; Hassig, C.; Wu, Y.; Ding, S.; Schultz, P. G. *Bioorg. Med. Chem. Lett.* **2004**, *14*, 449.
[41] Frey, R. R.; Wada, C. K.; Garland, R. B.; Curtin, M. L.; Michaelides, M. R.; Li, J.; Pease, L. J.; Glaser, K. B.; Marcotte, P. A.; Bouska, J. J.; Murphy, S. S.; Davidsen, S. K. *Bioorg. Med. Chem. Lett.* **2002**, *12*, 3443.
[42] Wada, C. K.; Frey, R. R.; Ji, Z.; Curtin, M. L.; Garland, R. B.; Holms, J. H.; Li, J.; Pease, L. J.; Guo, J.; Glaser, K. B.; Marcotte, P. A.; Richardson, P. L.; Murphy, S. S.; Bouska, J. J.; Tapang, P.; Magoc, T. J.; Albert, D. H.; Davidsen, S. K.; Michaelides, M. R. *Bioorg. Med. Chem. Lett.* **2003**, *13*, 3331.
[43] Vasudevan, A.; Ji, Z.; Frey, R. R.; Wada, C. K.; Steinman, D.; Heyman, H. R.; Guo, Y.; Curtin, M. L.; Guo, J.; Li, J.; Pease, L.; Glaser, K. B.; Marcotte, P. A.; Bouska, J. J.; Davidsen, S. K.; Michaelides, M. R. *Bioorg. Med. Chem. Lett.* **2003**, *13*, 3909.
[44] Curtin, M.; Glaser, K. *Curr. Med. Chem.* **2003**, *10*, 2373.
[45] Finnin, M. S.; Donigian, J. R.; Cohen, A.; Richon, V. M.; Rifkind, R. A.; Marks, P. A.; Breslow, R.; Pavletich, N. P. *Nature* **1999**, *401*, 188.
[46] Somoza, J. R.; Skene, R. J.; Katz, B. A.; Mol, C.; Ho, J. D.; Jennings, A. J.; Luong, C.; Arvai, A.; Buggy, J. J.; Chi, E.; Tang, J.; Sang, B.-C.; Verner, E.; Wynands, R.; Leahy, E. M.; Dougan, D. R.; Snell, G.; Navre, M.; Knuth, M. W.; Swanson, R. V.; McRee, D. E.; Tari, L. W. *Structure* **2004**, *12*, 1325.
[47] Vannini, A.; Volpari, C.; Filocamo, G.; Casavola, E. C.; Brunetti, M.; Renzoni, D.; Chakravarty, P.; Paolini, C.; Francesco, R. D.; Gallinari, P.; Steinkühler, C.; Marco, S. D. *Proc. Natl. Acad. Sci. U.S.A.*, **2004**, *101*, 15064.
[48] Christianson, D. W.; Lipscomb, W. N. *Acc. Chem. Res.* **1989**, *22*, 62.
[49] Kapstin, G. V.; Fejer, G.; Gronlund, J. L.; McCafferty, D. G.; Seto, E.; Etzkorn, F. A. *Org. Lett.* **2003**, *5*, 3053.
[50] Moree, W. J.; van der Marel, G. A.; Liskamp, R. M. J. *Tetrahedron Lett.* **1991**, *32*, 409.
[51] Christianson, D. W.; Lipscomb, W. N. *J. Am. Chem. Soc.* **1986**, *108*, 4998.
[52] Gagnard, V.; Leydet, A.; Morere, A.; Montero, J. -L.; Lefebvre, I.; Gosselin, G.; Pannecouque, C.; De Clercq, E. *Bioorg. Med. Chem.* **2004**, *12*, 1393.
[53] Barber, I.; Rayner, B.; Imbach, J.-L. *Bioorg. Med. Chem. Lett.* **1995**, *5*, 563.
[54] Matsuyama, A.; Yoshimatsu, Y.; Shimazu,T.; Sumida, Y.; Osada, H.; Komatsu, Y.; Nishino, N.; Khochbin, S.; Horinouchi, S.; Yoshida, M. *EMBO J.* **2002**, *21*, 6820.
[55] Koeller, K. M.; Haggarty, S. J.; Perkins, B. D.; Leykin, I.; Wong, J. C.; Kao, M. J.; Schreiber, S. L. *Chem. Biol.* **2003**, *10*, 397.
[56] Glaser, K. B.; Li, J.; Pease, L. J.; Staver, M. J.; Marcotte, P. A.; Guo, J.; Frey, R. R.; Garland, R. B.; Heyman, H. R.; Wada, C. K.; Vasudevan, A.; Michaelides, M. R.; Davidsen, S. K.; Curtin, M. L. *Biochem. Biophys. Res. Commun.*, **2004**, *325*, 683.
[57] Suzuki, T.; Miyata, N. *Curr. Med. Chem.* **2005**, *12*, 2867.

Received: July 15, 2005 **Revised: July 27, 2005** **Accepted: July 28, 2005**

Available online at www.sciencedirect.com
SCIENCE DIRECT
Bioorganic & Medicinal Chemistry Letters
ELSEVIER
Bioorganic & Medicinal Chemistry Letters 16 (2006) 3249–3254

Identification of novel PPARα ligands by the structural modification of a PPARγ ligand

Shinya Usui, Hiroki Fujieda, Takayoshi Suzuki, Naoaki Yoshida, Hidehiko Nakagawa and Naoki Miyata*

Graduate School of Pharmaceutical Sciences, Nagoya City University, 3-1 Tanabe-dori, Mizuho-ku, Nagoya, Aichi 467-8603, Japan

Received 2 February 2006; revised 1 March 2006; accepted 13 March 2006
Available online 18 April 2006

Abstract—To develop novel PPARα ligands, we designed and synthesized several 3-{3-[2-(nonylpyridin-2-ylamino)ethoxy]phenyl}-propanoic acid derivatives. Compound **10**, the meta isomer of a PPARγ agonist **1**, has been identified as a PPARα ligand. The introduction of methyl and ethyl groups at the C-2 position of the propanoic acid of **10** further improved the PPARα-binding potency.

Peroxisome proliferator-activated receptors (PPARs) belong to the nuclear receptor superfamily[1] and the PPAR subfamily consists of three members, PPARα, PPARγ, and PPARδ. These receptors act as ligand-activated transcription factors with other members of the nuclear receptor family,[2–4] and play a central role in the storage and catabolism of dietary fats by regulating the expression of a large number of genes involved in lipid metabolism and the energy balance.[5] PPARα is highly expressed in metabolically active tissues such as liver, heart, and muscle, and activation of PPARα decreases the serum triglyceride level and increases the HDL-c level.[6] Therefore, PPARα agonists such as clofibrate (Fig. 1) are being utilized as hypolipidemic agents. Meanwhile, PPARγ is expressed predominantly in adipose tissues and functions as a regulator of glucose and lipid homeostasis. The clinically useful thiazolidinedione (TZD) class of insulin sensitizers such as rosiglitazone[7] and pioglitazone[8] (Fig. 1) are potent PPARγ agonists used in the treatment of Type 2 diabetes. In addition, recent studies revealed that dual agonists of PPARα/γ decreased the free triglyceride plasma concentration and increased the plasma HDL concentration in an insulin resistant animal model.[9–11] Thus, many groups have ongoing research programs to find more potent and less toxic PPARα agonists and PPARα/γ dual agonists.

We previously reported compound **1**, which was designed based on the structure of rosiglitazone and 15d-PGJ_2,[12,13] as a potent PPARγ ligand.[14] To find novel PPARα agonists, we chose compound **1** as a lead structure, because recent reports on selective PPAR ligands indicated that minor structural modifications can affect selectivity.[15–17] In this letter, we report the design, synthesis, and binding affinity of PPAR ligands based on the structure of compound **1**.

In the course of our computational studies on compound **1** and its derivatives using Glide 3.5 software, we found that compound **10** (Fig. 2), the meta isomer of **1**, likely fits PPARα protein more tightly than **1**.[18] An inspection of the simulated PPARα/**1** complex showed that one of the two oxygen atoms of the carboxylate group forms hydrogen bonds with His 440 and Tyr 464, and that the nonyl group is located in the hydrophobic region formed by Ile 241, Leu 247, Ala 250, Leu 254, Ile 272, Val 332, and Ala 333 (Fig. 3, left). In the simulated PPARα/**10** complex, as well as the hydrogen bonds and the hydrophobic interaction found in the PPARα/**1** complex, the existence of added hydrogen bonds was expected between the other oxygen atom of the carboxylate and Ser 280, and between the tertiary nitrogen and Thr 279 (Fig. 3, right). These results prompted us to evaluate the affinity for PPAR of **10** and its derivatives **2–9** and **11–20** (Fig. 2).

Keywords: Peroxisome proliferator-activated receptor; PPARα ligand; PPARγ ligand; Nuclear receptor.
* Corresponding author. Tel./fax: +81 52 836 3407; e-mail: miyata-n@phar.nagoya-cu.ac.jp

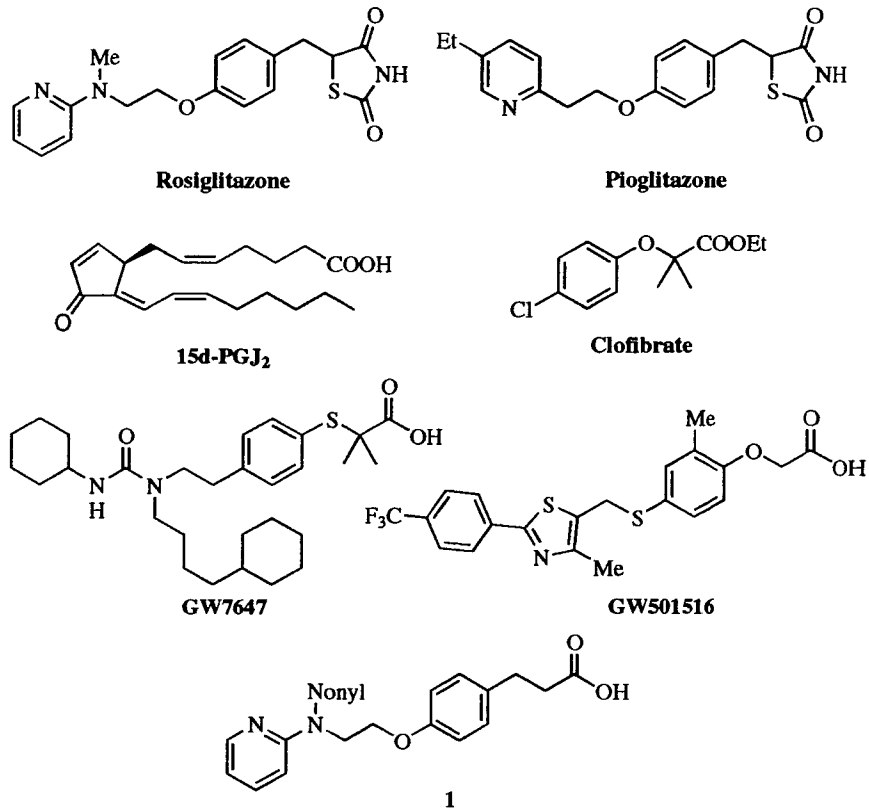

Figure 1. Structures of rosiglitazone, pioglitazone, 15d-PGJ_2, clofibrate, GW7647, GW501516, and compound **1**.

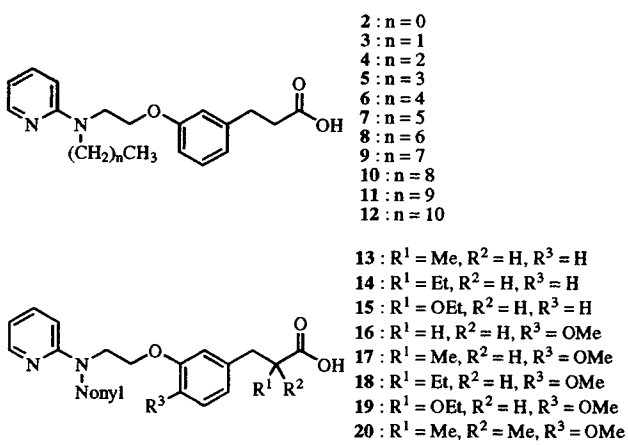

Figure 2. Structures of compounds **2–20**.

The compounds prepared for this study are shown in Figure 2, and the routes used for their synthesis are illustrated in Schemes 1 and 2. Scheme 1 shows the preparation of the 3-{3-[2-(alkylpyridin-2-ylamino)ethoxy]phenyl}propanoic acid derivatives **2–16**, **18**, and **19**. The yield of 2-alkylaminopyridine **22a–k** was 69–86%, using the method of Buchwald:[19] treatment of 2-bromopyridine **21** with *n*-nonylamine (4 equiv), $Pd_2(DBA)_3$, BINAP, and *t*-BuONa in toluene under reflux. *m*-Hydroxybenzaldehyde **23a** and isovaniline **23b** were allowed to react with 1,2-dibromoethane to give ethers **24a** and **24b**. The Horner–Wadsworth–Emmons reaction[20] was applied to the conversion of **24a, b** into acrylic acid derivatives **25a–g**. The double bond of **25a–g** was hydrogenated to yield compounds **26a–g**. Coupling between 2-alkylaminopyridine **22a–k** and propanoic acid ethyl esters **26a** afforded *N*-(2-pyridinyl)-*N*-alkylpropanoic acids **27a–k**. Propanoic acid ethyl esters **26b–g** were also allowed to react with 2-nonylaminopyridine **22i** to afford *N*-(2-pyridinyl)-*N*-nonylpropanoic acids **27l–q**. The subsequent hydrolysis of **27a–q** gave the desired carboxylic acids **2–16**, **18**, and **19**.

The preparation of 3-{4-methoxy-3-[2-(nonylpyridin-2-ylamino)ethoxy]phenyl}propanoic acids **17** and **20**, which have one or two methyl groups at the C-2 position of the propanoic acid, is outlined in Scheme 2. The aldehyde **24b** was reduced by $NaBH_4$ and allowed to react with acetic anhydride to give acetic acid 3-(2-bromoethoxy)benzyl ester **29**. Compound **29** was treated with 1-methoxy-1-trimethylsilyloxypropene or dimethylketene methyltrimethylsilyl acetal in the presence of magnesium perchlorate in anhydrous CH_2Cl_2 to give esters **30a,b**.[21] Coupling between 2-nonylaminopyridine **22i** and propanoic acid methyl esters **30a,b** afforded *N*-(2-pyridinyl)-*N*-nonyl compounds **31a,b** and subsequent hydrolysis gave carboxylic acids **17** and **20**.

The binding affinity of the compounds for PPARs was evaluated with a CoA-BAP System (Microsystems).[22] In this system, the alkaline phosphatase (AP) activity is directly proportional to the affinity of the ligands for PPARs.

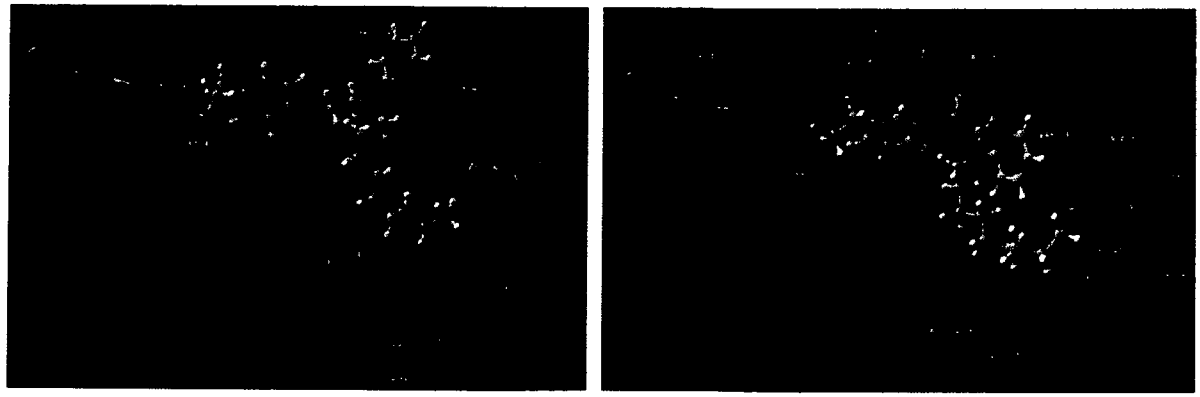

Figure 3. View of the lowest energy conformations of 1 (left) and **10** (right) docked in PPARα. Residues around compounds and hydrogen bonds are displayed as wires and dotted lines, respectively. Figures represent distances in angstrom.

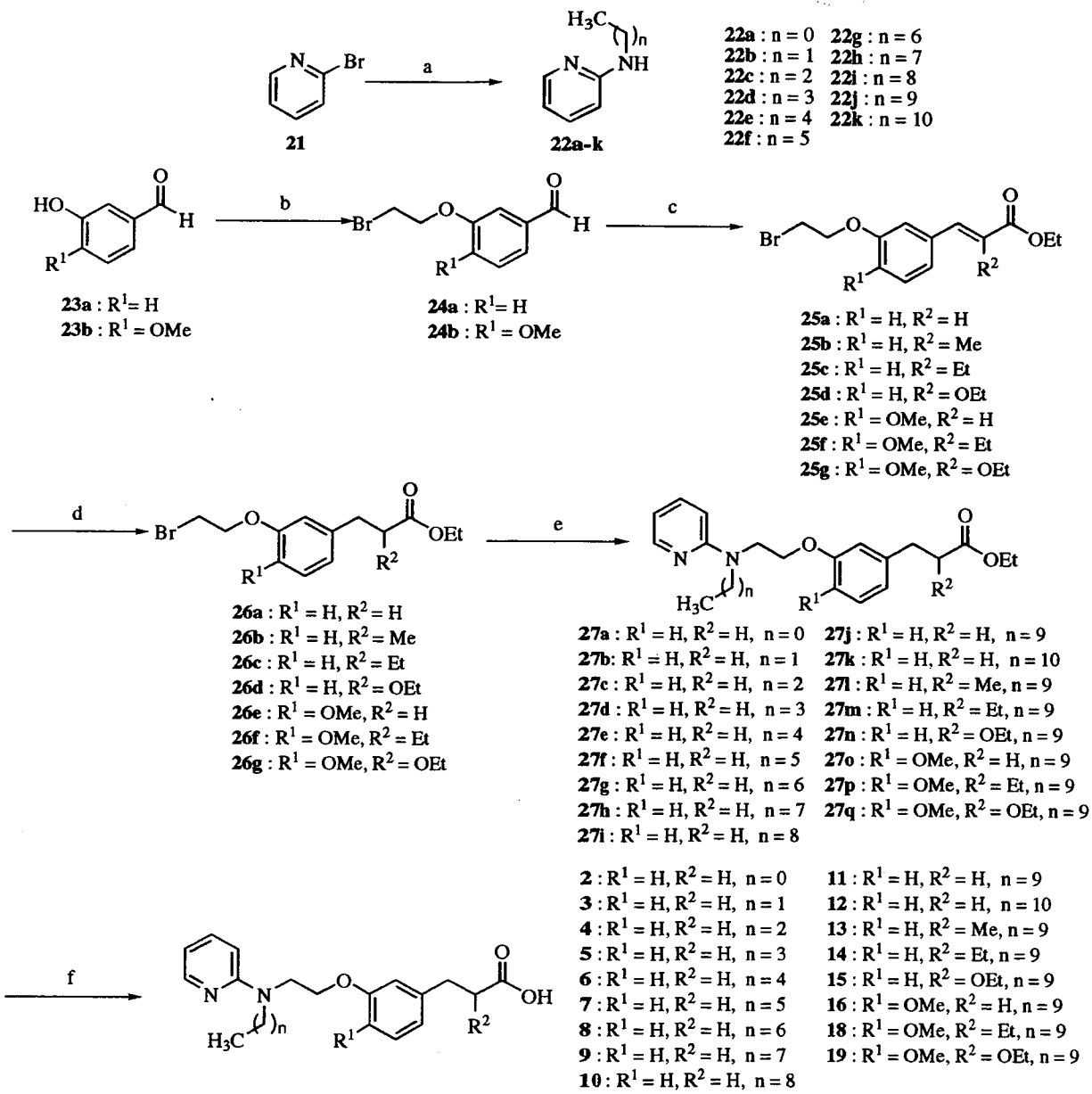

Scheme 1. Reagents and conditions: (a) $CH_3(CH_2)_nNH_2$, $Pd_2(DBA)_3$, BINAP, *t*-BuOH, toluene, 80 °C, 69–86%; (b) 1,2-dibromoethane, Cs_2CO_3, THF, 65 °C, 40–57%; (c) $(EtO)_2P(O)CH(R^2)CO_2Et$, NaH, anhydrous THF, 0 °C to rt, 47–95%; (d) H_2, Pd/C, EtOH, 79–97%; (e) **22a–k**, Et_3N, KI, 105 °C, 7–14%; (f) aq NaOH, EtOH–THF, rt, 89–95%.

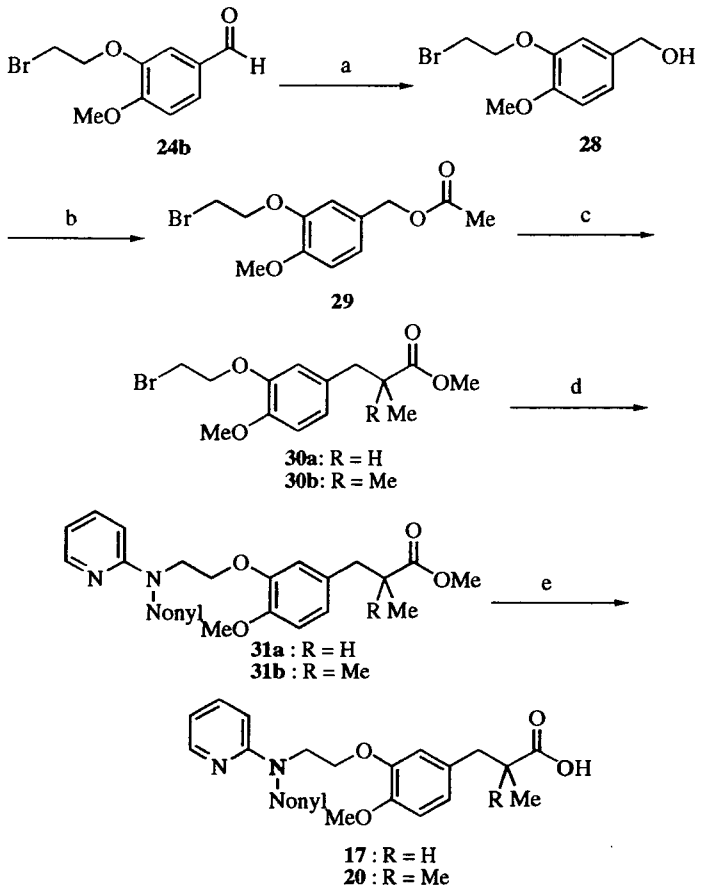

Scheme 2. Reagents and conditions: (a) $NaBH_4$, EtOH, rt, 97%; (b) Ac_2O, DMAP, rt, 96%; (c) 1-methoxy-1-trimethylsilyloxypropene or dimethylketene methyltrimethyl silyl acetal, $Mg(ClO_4)_2$, rt, 94–95%; (d) **22i**, Et_3N, KI, 105 °C, 5–13%; (e) aq NaOH, EtOH, rt, 75–76%.

The ability of compounds **2–20** to bind PPARα, PPARγ, and PPARδ was evaluated and the results are shown in Tables 1–3, respectively. GW7647[23] (PPARα), rosiglitazone[7] (PPARγ), and GW501516[24] (PPARδ) were used as reference compounds (Fig. 1). The lead compound **1** showed high affinity for PPARγ and little affinity for PPARα and PPARδ (Tables 1–3, line 1). As we had expected from the computational study described above,

Table 1. Binding affinity for PPARα of compounds **1–20** at 0.1, 1.0, and 10 μM

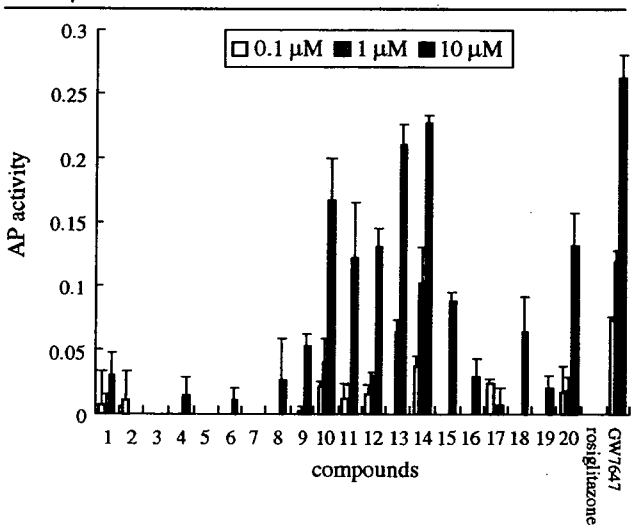

Values are means of at least three experiments.

Table 2. Binding affinity for PPARγ of compounds **1–20** at 0.1, 1.0, and 10 μM

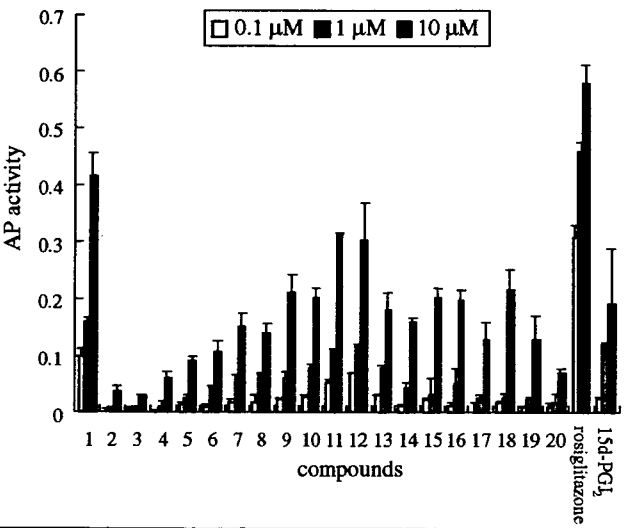

Values are means of at least three experiments.

Table 3. Binding affinity for PPARδ of compounds **1–20** at 0.1, 1.0, and 10 μM

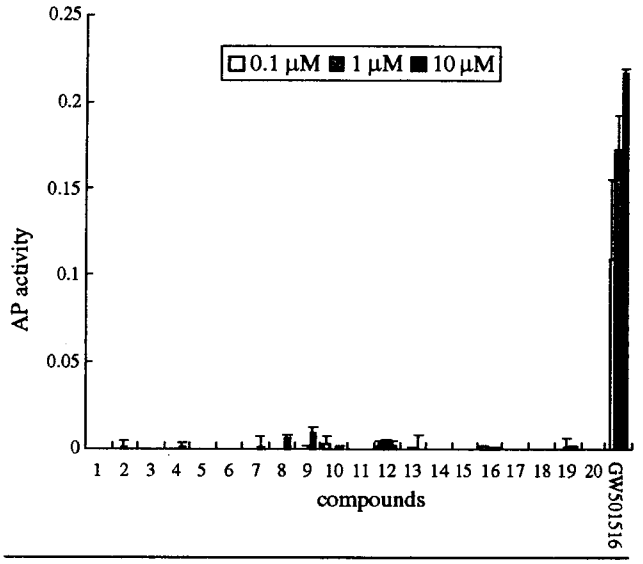

Values are means of at least three experiments.

compound **10**, the meta isomer of compound **1**, displayed much higher affinity for PPARα than did **1** (Table 1, line 1 vs 10). Furthermore, the affinity for PPARγ of **10** is lower than that of **1** (Table 2, line 1 vs 10), and compound **10** exhibited no affinity for PPARδ (Table 3, line 10).

To study the structure–activity relationship of 3-{3-[2-(alkylpyridin-2-ylamino)ethoxy]phenyl}propanoic acid derivatives and to find more potent PPARα ligands, we initially evaluated the PPAR-binding affinity of compounds **2–12** which have alkyl chains of various lengths on their nitrogen atom. It was found that the affinity of these compounds was closely related to chain length. Among compounds **2–12**, nonyl **10** showed the greatest affinity for PPARα, while decyl **11** and undecyl **12** were most active toward PPARγ, and heptyl **8** and octyl **9** showed little affinity for PPARδ (Tables 1–3, lines 2–12).

We next examined the effect of substituents at the C-2 position of the propanoic acid of **10**, because it has been reported that the introduction of an alkyl or alkoxy group at this position increases activity for PPARα.[15,25–27] Methyl **13**, ethyl **14**, and ethoxy **15** were tested, and much to our satisfaction, **13** and **14** showed strong affinity for PPARα and slightly weak affinity for PPARγ as compared with the parent compound **10**. In addition, compounds **13–15** had no affinity for PPARδ (Tables 1–3, lines 13–15).

To examine the effect of the introduction of a methoxy group at the C-4 position of the benzene ring, compounds **16–20** were investigated. However, these compounds did not show a pronounced affinity for PPARα compared to compounds **10**, **13**, and **14** (Tables 1, lines 16–20).

In summary, to find novel PPARα ligands, we prepared several 3-{3-(2-nonylaminoethoxy)phenyl}propanoic acid derivatives which were designed based on the structure of the PPARγ agonist **1**. Compound **10**, the meta isomer of **1**, was found to be a PPARα ligand. The introduction of methyl (**13**) and ethyl (**14**) groups at the C-2 position of the propanoic acid of **10** further improved the PPARα-binding potency. The findings of this study will help provide an effective agent for hyperlipidemia. Currently, further detailed studies pertaining to compounds **13** and **14** are under way.

References and notes

1. Nuclear Receptors Nomenclature Committee. *Cell* **1999**, *97*, 161.
2. Willson, T. M.; Brown, P. J.; Sternbach, D. D.; Henke, B. R. *J. Med. Chem.* **2000**, *43*, 527.
3. Willson, T. M.; Cobb, J. E.; Cowan, D. J.; Wiethe, R. W.; Correa, I. D.; Prakash, S. R.; Beck, K. D.; Moore, L. B.; Kliewer, S. A.; Lehmann, J. M. *J. Med. Chem.* **1996**, *39*, 665.
4. Kersten, S.; Desvergne, B.; Wahli, W. *Nature* **2000**, *405*, 421.
5. Bogacka, I.; Xie, H.; Bray, G. A.; Smith, S. R. *Diabetes Care* **2004**, *27*, 1660.
6. Francis, G. A.; Annicotte, J. S.; Auwerx, J. *Curr. Opin. Pharmacol.* **2003**, *3*, 186.
7. Cantello, B. C. C.; Cawthorone, M. A.; Cottam, G. P.; Duff, P. T.; Haigh, D.; Hindley, R. M.; Lister, C. A.; Smith, S. A.; Thurlby, P. L. *J. Med. Chem.* **1994**, *37*, 3977.
8. Momose, Y.; Meguro, K.; Ikeda, H.; Hatanaka, C.; Oi, S.; Sohda, T. *Chem. Pharm. Bull.* **1991**, *39*, 1440.
9. Lohray, B. B.; Lohray, V. B.; Bajji, A. C.; Kalchar, S.; Poondra, R. R.; Padakanti, S.; Chakrabarti, R.; Vikramadithyan, R. K.; Misra, P.; Juluri, S.; Mamidi, N. V.; Rajagopalan, R. *J. Med. Chem.* **2001**, *44*, 2675.
10. Duran-Sandoval, D.; Thomas, A. C.; Bailleul, B.; Fruchart, J. C.; Staels, B. *Med. Sci.* **2003**, *19*, 819.
11. Henke, B. R. *J. Med. Chem.* **2004**, *47*, 4118.
12. Forman, B. M.; Tontonoz, P.; Chen, J.; Brun, R. P.; Spiegelman, B. M.; Evans, R. M. *Cell* **1995**, *83*, 803.
13. Kliewer, S. A.; Lenhard, J. M.; Willson, T. M.; Patel, I.; Morris, D. C.; Lehmann, J. M. *Cell* **1995**, *83*, 813.
14. Usui, S.; Suzuki, T.; Hattori, Y.; Etoh, K.; Fujieda, H.; Nishizuka, M.; Imagawa, M.; Nakagawa, H.; Kohda, K.; Miyata, N. *Bioorg. Med. Chem. Lett.* **2005**, *15*, 1547.
15. Nomura, M.; Tanase, T.; Ide, T.; Tsunoda, M.; Suzuki, M.; Uchiki, H.; Murakami, K.; Miyachi, H. *J. Med. Chem.* **2003**, *46*, 3581.
16. Weigand, S.; Bischoff, H.; Dittrich-Wengenroth, E.; Heckroth, H.; Lang, D.; Vaupel, A.; Woltering, M. *Bioorg. Med. Chem. Lett.* **2005**, *15*, 4619.
17. Kasuga, J.; Makishima, M.; Hashimoto, Y.; Miyachi, H. *Bioorg. Med. Chem. Lett.* **2006**, *16*, 554.
18. The X-ray structure of PPARα complexed with GW409544 was taken from the Brookhaven Protein Data Bank (PDB code 1K7L). The protein was prepared for docking, using the protein preparation and refinement utility provided by Glide 3.5 software. Water molecules of crystallization were removed from the complexes, and hydrogen atoms were added computationally at appropriate positions. Calculations of docking between the prepared PPARα protein and compound **2** or **10** were performed using Glide 3.5 software.
19. Wagaw, S.; Buchwald, S. L. *J. Org. Chem.* **1996**, *61*, 7240.
20. Maryanoff, B. E.; Reitz, A. B. *Chem. Rev.* **1989**, *89*, 863.
21. Grieco, P. A.; Handy, S. T. *Tetrahedron Lett.* **1997**, *38*, 2645.
22. Kanayama, T.; Mamiya, S.; Nishihara, T.; Nishikawa, J. *J. Biochem.* **2003**, *133*, 791.

23. Brown, P. J.; Stuart, L. W.; Hurley, K. P.; Lewis, M. C.; Winegar, D. A.; Wilson, J. G.; Wilkison, W. O.; Ittoop, O. R.; Willson, T. M. *Bioorg. Med. Chem. Lett.* **2001**, *11*, 1225.
24. Sznaidman, M. L.; Haffner, C. D.; Maloney, P. R.; Fivush, A.; Chao, E.; Goreham, D.; Sierra, M. L.; LeGrumelec, C.; Xu, H. E.; Montana, V. G.; Lambert, M. H.; Willson, T. M.; Oliver, W. R., Jr.; Sternbach, D. D. *Bioorg. Med. Chem. Lett.* **2003**, *13*, 1517.
25. Lowe, D. B.; Bifulco, N.; Bullock, W. H.; Claus, T.; Coish, P.; Dai, M.; Dela Cruz, F. E.; Dickson, D.; Fan, D.; Hoover-Litty, H.; Li, T.; Ma, X.; Mannelly, G.; Monahan, M. K.; Muegge, I.; O'Connor, S.; Rodriguez, M.; Shelekhin, T.; Stolle, A.; Sweet, L.; Wang, M.; Wang, Y.; Zhang, C.; Zhang, H. J.; Zhang, M.; Zhao, K.; Zhao, Q.; Zhu, J.; Zhu, L.; Tsutsumi, M. *Bioorg. Med. Chem. Lett.* **2006**, *16*, 297.
26. Koyama, H.; Boueres, J. K.; Miller, D. J.; Berger, J. P.; MacNaul, K. L.; Wang, P. R.; Ippolito, M. C.; Wright, S. D.; Agrawal, A. K.; Moller, D. E.; Sahoo, S. P. *Bioorg. Med. Chem. Lett.* **2005**, *15*, 3347.
27. Koyama, H.; Miller, D. J.; Boueres, J. K.; Desai, R. C.; Jones, A. B.; Berger, J. P.; MacNaul, K. L.; Kelly, L. J.; Doebber, T. W.; Wu, M. S.; Zhou, G.; Wang, P. R.; Ippolito, M. C.; Chao, Y. S.; Agrawal, A. K.; Franklin, R.; Heck, J. V.; Wright, S. D.; Moller, D. E.; Sahoo, S. P. *J. Med. Chem.* **2004**, *47*, 3255.

Highly Potent and Selective Histone Deacetylase 6 Inhibitors Designed Based on a Small-Molecular Substrate

Takayoshi Suzuki, Akiyasu Kouketsu, Yukihiro Itoh, Shinya Hisakawa, Satoko Maeda, Minoru Yoshida, Hidehiko Nakagawa, and Naoki Miyata

Graduate School of Pharmaceutical Sciences, Nagoya City University, 3-1 Tanabe-dori, Mizuho-ku, Nagoya, Aichi 467-8603, Japan, RIKEN, Saitama 351-0198, Japan, and CREST Research Project, Japan Science and Technology Agency, Saitama 332-001, Japan

JOURNAL OF
MEDICINAL CHEMISTRY®

Reprinted from
Volume 49, Number 16, Pages 4809–4812